

## 3D Path Planning Based on Probabilistic Foam for UAV Indoor Applications<sup>\*</sup>

Luís B. P. Nascimento<sup>\*,\*\*</sup> Vitor G. Santos<sup>\*,\*\*</sup> Diego S. Pereira<sup>\*,\*\*</sup>  
Pablo J. Alsina<sup>\*\*</sup>

<sup>\*</sup> *Federal Institute of Rio Grande do Norte, Parnamirim, Brazil*  
(e-mail: lbruno@ufrn.edu.br, {vitor.gaboardi,  
diego.pereira}@ufrn.edu.br).

<sup>\*\*</sup> *Federal University of Rio Grande do Norte, Natal, 59078-970, Brazil*  
(e-mail: pablo@dca.ufrn.br)

---

**Abstract:** The recent growth of the Unmanned Aerial Vehicle (UAV) industry stimulated research development to solve different problems, such as inspection in hard-to-reach places, mapping, and search and rescue. Frequently, these applications require navigation in indoor environments, so searching for safe paths for the UAVs to fly is essential for mission accomplishment. In this context, we propose in this paper the employment of the Goal-Biased Probabilistic Foam (GBPF) method to perform the path planning for a UAV in indoor missions. The GBPF method ensures a fast search of a path with a safe region provided by a structure called bubble that will be modeled for the UAV. The bubble represents a free-space region that allows safe UAV maneuvers, decreasing the probability of obstacles collision. To validate the proposed methodology, we used the Virtual Robot Experimentation Platform (V-REP) to simulate an UAV flight in an indoor environment using the path generated by the GBPF.

*Keywords:* UAV; Probabilistic Foam; Path Planning; Bubble of Free Space; V-REP.

---

### 1. INTRODUCTION

In recent years, many researches related to Unmanned Aerial Vehicle (UAV), also known as drones, were developed, showing the potential that this aeronautical technology can offer in different applications (Zhao et al., 2018). Among them, it is possible to highlight the usage of UAVs on tasks of inspection in hard-to-reach places, such as wind turbines, power transmission towers, bridges, and solar panels (Shakeri et al., 2019), surveillance system (Jung et al., 2018), assistance in monitoring plantations (Ju and Son, 2018) and ocean (Ma et al., 2020).

On the other hand, indoor applications with UAVs are more complex than the outdoor ones, mainly because of the restrictions imposed by the autonomous navigation system of the aircraft, such as communications limitations and proximity to obstacles, where, in case of collision, it may endanger the aircraft integrity, completeness of the mission and even human lives (Grzonka et al., 2009).

An example of these indoor applications was discussed by La Scalea et al. (2019), where they mention the possibility of using drones for cave exploration. In Zhang et al. (2017), the authors present a solution called SmartCaveDrone, a system capable of mapping caves in 3D models. Furthermore, in McCabe et al. (2017), the authors detail the benefits that UAVs can bring to monitoring construction works in civil construction.

The usage of UAVs in diverse applications is growing up fast, and for the development of this technology, it is necessary to look for solutions that integrate these aircraft with environments that are becoming increasingly complex, making UAV systems more resilient, reliable, and improving their capabilities.

Path planning is one of the main issues in autonomous navigation, and it has been debated in the scientific community since the 1980s (Chien et al., 1984; Canny, 1988; Takahashi and Schilling, 1989). The planning is particularly relevant since it is practically a requirement for an autonomous mobile robot to move from an initial to a goal configuration, avoiding collisions in an environment with obstacles and narrow passages (LaValle, 2006).

Most path planning techniques have the purpose of creating optimal paths or finding feasible paths with low running time (Volna and Kotyrba, 2018). However, it is also important to guarantee safety for a robot when moving in unstructured environments (Plaku et al., 2018). Thus, planning paths sufficiently far from the obstacles is crucial for most applications (Berglund et al., 2009). Besides, when considering an indoor mission for a UAV, it is essential to incorporate techniques in which it can avoid collisions so that there is no physical damage to the robot. Aggarwal and Kumar (2020).

Proposed in (Nascimento et al., 2018b), Goal-Biased Probabilistic Foam (GBPF) is an interesting global path planning method capable of providing short paths with safe regions for maneuverability. Therefore, in this paper, we

---

<sup>\*</sup> This study was financed in part by the Coordenação de Aperfeiçoamento de Pessoal de Nível Superior - Brasil (CAPES) - Finance Code 001.

present the application of GBPF method for a UAV to accomplish indoor missions safely.

This paper is organized as follows: Section 2 introduces the UAV modeling that was used in the path planning method. Section 3 describes the Goal-biased Probabilistic Foam, a variant method of the original PFM. Section 4 presents simulation results and discussions. Finally, Section 5 discusses conclusions and future works.

## 2. BUBBLE MODELING FOR UAV

The concept of *bubbles of free-space*, proposed by Quinlan (1995), makes possible the computation of a volumetric collision-free region in C-space  $C$  around a robot configuration  $q$  based on distance information in workspace  $W$ . This region, called bubble, will be used by our path planner to provide safe paths.

Let us consider for the experiments a quadrotor UAV denoted by  $A$ . Disregarding the rotational degrees of freedom (DoF), the robot  $A$  will present three translational DoF, denoted by  $X$ ,  $Y$ , and  $Z$ , as can be seen in Figure 1.

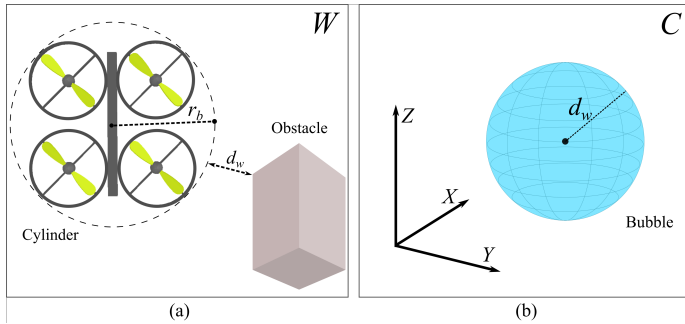


Figure 1. Bubble modeling. (a) Measuring the minimum distance between the obstacle and the cylinder which encloses the UAV in workspace  $W$ . (b) The bubble computed in C-space  $C$ .

Figure 1a illustrates an environment with the UAV and an obstacle, representing the workspace  $W$ . Also, let us consider that the robot is inscribed in a cylinder that contains the entire robot. The measure  $d_w$  is the minimum distance between the cylinder and the obstacles.

Now, let us consider moving the UAV from configurations  $q$  to  $p$  along a straight line, where the distance traveled by the UAV will be  $\|q - p\|$ . If the UAV moves a distance no greater than  $d_w$ , it will not collide with any obstacles or walls in the environment. The bubble, as can be seen in Figure 1b, is a volumetric region in free C-space, which represents the set of all these configurations  $p$ .

More formally, the bubble is defined as a  $n$ -ball with radius  $d_w$ , centered in configuration  $q$ .

$$B(q) = \{p : \|q - p\| \leq d_w\} \quad (1)$$

In Quinlan (1995), this region  $B$  was proposed for general non-rotating free-flying robots in planar environments. In this work, we apply this concept to a UAV robot, which will navigate using a path planning method based on Probabilistic Foam.

## 3. GOAL-BIASED PROBABILISTIC FOAM

The method Goal-Biased Probabilistic Foam (Nascimento et al., 2018b) is a global sampling-based path planner ideal for robots that need to perform safe motion. The GBPF is a variant of the Probabilistic Foam Method (Nascimento et al., 2018a, 2020) where bubbles are expanded in the free configuration space and propagate with a strategy inspired on the expanding method of the search tree from the RRT-GoalBias algorithm Lavelle et al. (2000), a variant of the classic Rapidly-Exploring Random Tree (RRT) LaValle (1998). The method GBPF converges to the goal configuration faster than the original PFM and provides paths with high clearance, differently from RRT. The propagation process of GBPF is shown in Figure 2

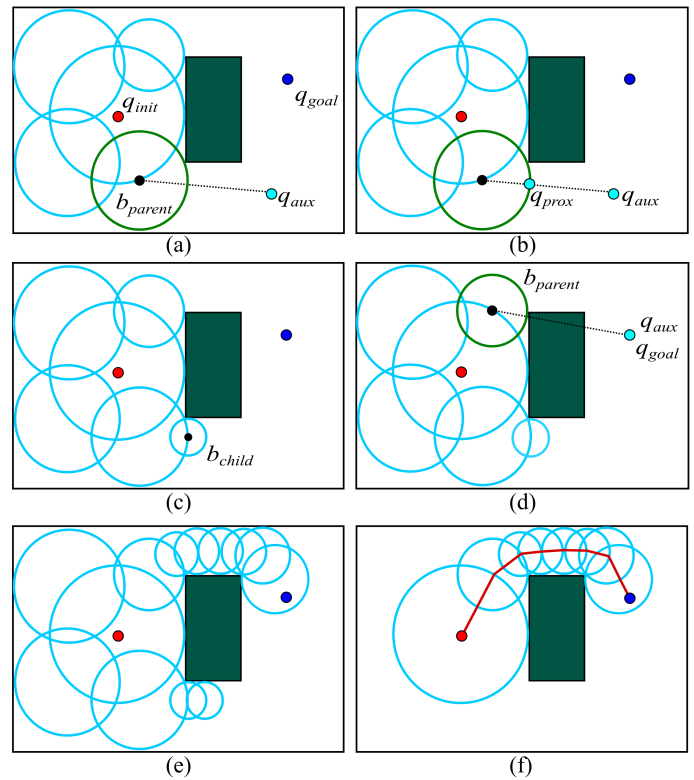


Figure 2. GBPF propagation. (a) Selection of a parent bubble (green circle). (b) Find the new child bubble center  $q_{prox}$ . (c) Child bubble expanded. (d) Biased selection of  $b_{parent}$ . (e) Probabilistic foam. (f) Rosary found and path extracted (red line).

During the foam propagation process, a configuration  $q_{aux}$  is sampled in the configuration space and the bubble with the center closest to configuration  $q_{aux}$  is selected as parent bubble  $b_{parent}$  (Figure 2a). Next, the configuration  $q_{near}$  is found on the surface of the bubble  $b_{parent}$  (Figure 2b), and then, a new child bubble  $b_{child}$  centered in  $q_{near}$  is expanded (Figure 2c), finishing a generation.

The method tends to propagate the foam towards to  $q_{goal}$  due to the bias, defined as a small probability (such as 0.05, as suggested by Lavelle et al. (2000)) for the auxiliary configuration  $q_{aux}$  to be sampled on the goal configuration. Figure 2d illustrates this bias configuration in the propagation process. In this way, the next parent bubble will be the bubble with the center closest to  $q_{goal}$ .

This process repeats until a bubble encloses the goal configuration, ending the propagation of the probabilistic foam, as seen in Figure 2e. Finally, the Rosary  $\mathcal{R}$ , shown in Figure 2f, is the sequence of overlapped bubbles from  $q_{goal}$  to  $q_{init}$ , following the parentship relation between bubbles. The resulted path can be easily extracted from the rosary.

### 3.1 GBPF pseudocode

The pseudocode of the Goal-biased Probabilistic Foam method is described in Algorithm 1.

---

#### Algorithm 1 Goal-biased Probabilistic Foam

---

**Input:**  $q_{init}, q_{goal}, r_{min}, bias$

**Output:**  $\mathcal{R}$

```

1:  $F = \emptyset$ 
2:  $r \leftarrow \text{expand\_bubble}(q_{init})$ 
3:  $F.add(\{q_{init}, r\})$ 
4: while  $\mathcal{R} = \emptyset$  do
5:   if  $\text{rand}() > bias$  then
6:      $q_{aux} \leftarrow \text{random\_config}()$ 
7:   else
8:      $q_{aux} \leftarrow q_{goal}$ ;
9:   end if
10:   $\{q_p, r_p\} \leftarrow \text{nearest\_bubble}(q_{aux}, F)$ 
11:   $q_{near} \leftarrow \text{nearest\_config}(q_p, r_p, q_{aux})$ 
12:  if  $\text{interior}(q_{near}, F) = \text{false}$  then
13:     $r_{near} \leftarrow \text{expand\_bubble}(q_{near})$ 
14:    if  $r_{near} \geq r_{min}$  then
15:       $F.add(\{q_{near}, r_i\})$ 
16:      if  $\|q_{near} - q_{goal}\| \leq r_{near}$  then
17:         $\mathcal{R} \leftarrow F.get\_rosary()$ 
18:        return success
19:      end if
20:    end if
21:  end if
22: end while

```

---

The method described in Algorithm 1 receives as input  $q_{init}, q_{goal}, r_{min}$ , the value of  $bias$ , and returns the rosary  $\mathcal{R}$ . In *line 2* the first bubble is expanded using the function  $\text{expand\_bubble}()$ , and it is added in the foam  $F$ . At *lines 5-9* occurs the sampling of  $q_{aux}$ . The function  $\text{rand}()$  returns a uniform random value between  $[0,1]$ .

The function  $\text{nearest\_bubble}(q_{aux}, F)$  obtains the bubble (center and radius) inside  $F$  with the nearest center to  $q_{aux}$ . The function  $\text{nearest\_config}(q_p, r_p, q_{aux})$  returns the nearest point  $q_{near}$  between the surface of this bubble and the configuration  $q_{aux}$  (*lines 10 and 11*). If  $q_{near}$  was not sampled in the interior of another bubble in  $F$  (verification using the function  $\text{interior}()$  at *line 11*), a new bubble is expanded (*line 12*). If the radius of the new bubble is greater or equal to  $r_{min}$ , this bubble is stored in  $F$ . The method GBPF runs while the rosary  $\mathcal{R}$  is not found. Other stopping criteria that can be considered are the execution time and the total number of computed bubbles.

### 3.2 Path smoothing

The path obtained by GBPF is bounded by a sequence of overlapped bubbles (rosary) that provide safety constraints. An interesting advantage of this region is that the path remains safe while it crosses all bubbles from

the rosary through the intersection region between two consecutive bubbles. Therefore, this feature can be used to perform path adjustments and, consequently, smooth the resulted path. Nascimento et al. (2020) present an optimization approach to smooth the path obtained by path planners based on the probabilistic foam. We use the same approach in this work to make the path smoother.

## 4. RESULTS

To test the methodology presented in this paper, we created a simulation environment in the Virtual Robot Experimentation Platform software, also known as V-REP<sup>1</sup>. This scenario represents a two-floored house, as shown in Figure 3. Furthermore, we used the quadricopter mobile robot available in V-REP as UAV to follow the planned path by the Probabilistic Foam Method, which was generated using MATLAB.

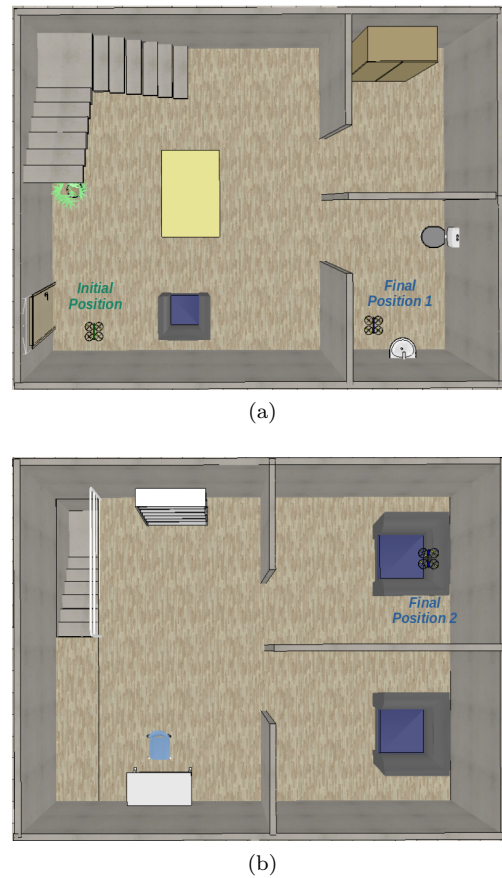


Figure 3. Scenario created in V-REP: (a) First floor with initial (green) and final (blue) UAV position for Simulation 1. (b) Second floor with the final UAV position for Simulation 2.

In this paper, we created two experiments that represent an indoor mission. In Experiment 1, the UAV will navigate only in the first floor, from configuration  $q_{init} = [5.5, 1, 0.5]$  m to  $q_{goal} = [5.4, 6.4, 0.5]$  m. These configurations  $q_{init}$  and  $q_{goal}$  are represented by Initial Position and Final Position 1 in Figure 3a, respectively.

In Experiment 2, the UAV will navigate from the first to the second floor, i.e., from  $q_{init} = [5.5, 1, 0.5]$  m,

<sup>1</sup> <https://www.coppeliarobotics.com/>

represented by Initial Position in Figure 3a, to  $q_{goal} = [1.5, 7, 4.3]$ , represented by Final Position 2 in Figure 3b.

The experiments were performed on a 1.8 GHz Intel Core i7 with 8 GB RAM. The GBPF parameters were  $r_{min} = 0.08$  m and  $bias = 0.05$ . These values were defined empirically by testing different configurations and choosing the best results. The radius of the cylinder (Figure 1) used for computing bubbles is  $r_b = 0.2$  m, which was chosen based on the UAV geometry available in V-REP. The path planning with GBPF for Experiment 1 is presented in Figure 4.

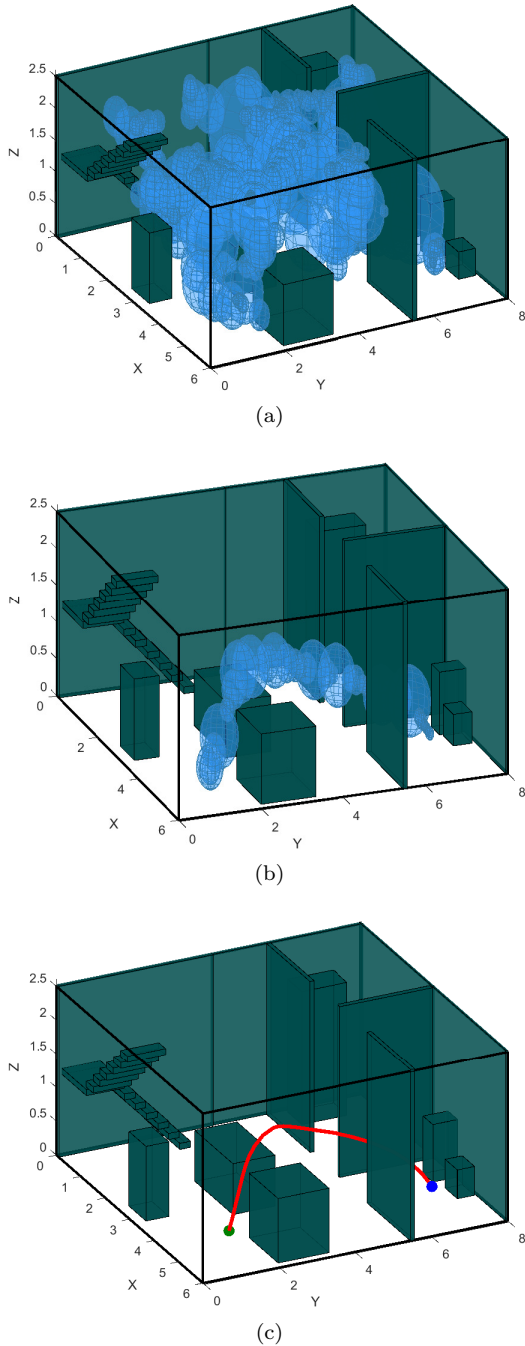


Figure 4. Path Planning in 1st Floor (a) Probabilistic Foam. (b) Rosary. (c) Planned Path from initial (green dot) to goal (blue dot) configurations.

In this first experiment where only the first floor was considered, GBPF found a feasible path in 0.8321 seconds with a total of 185 computed bubbles.

The GBPF path planning for Experiment 2 is presented in Figure 5.

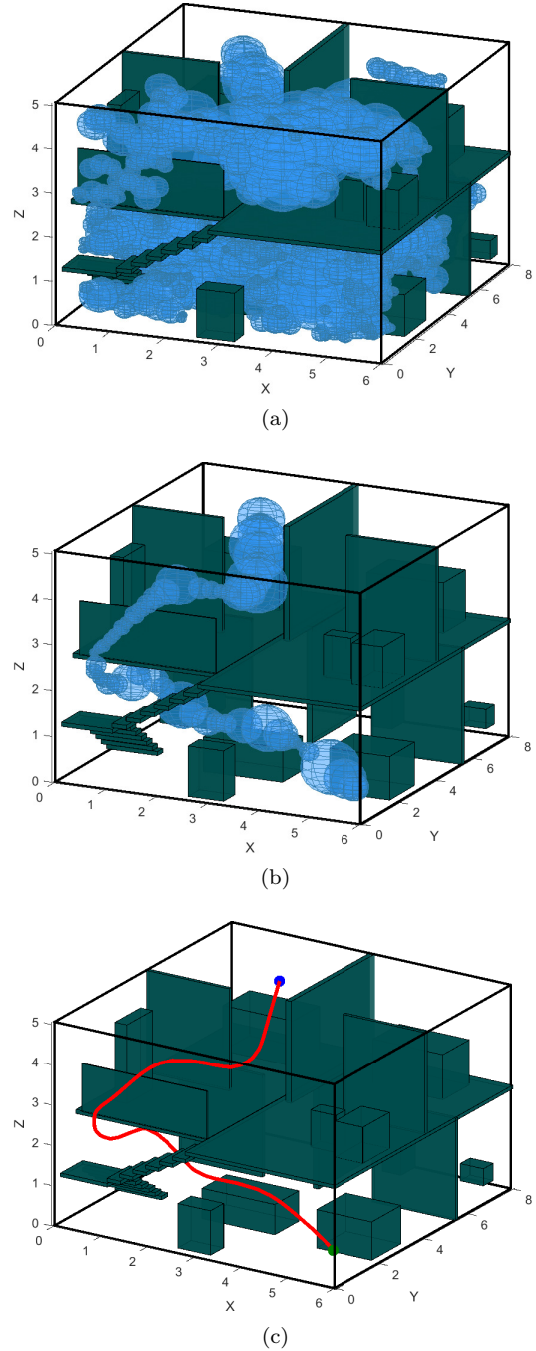


Figure 5. Path Planning from 1st to 2nd Floor (a) probabilistic Foam. (b) Rosary formed. (c) Planned Path from initial (green dot) to goal (blue dot) configurations.

For the second experiment where the first and second floors were considered, GBPF found a feasible path in 1.3661 seconds with a total of 873 computed bubbles. The number of computed bubbles and the search time were higher than the values from experiment 1, which is expected, since the environment is more complex.

An approximated representation of the realistic environment in V-REP was created in MATLAB considering only simple cuboids in order to facilitate the computation of the path planning. However, it is important to observe that it was not necessary to compute the region of the obstacles in the configuration space (C-obstacle) for the calculation of the bubble, which is an important advantage of the presented bubble modeling.

Finally, the application of the paths obtained for experiments 1 and 2 with the UAVs in V-REP is presented in Figures 6 and 7, respectively. Additionally, a demonstrative video with the experiments' results is available and can be seen on <https://youtu.be/f68tPGB0HTk>.

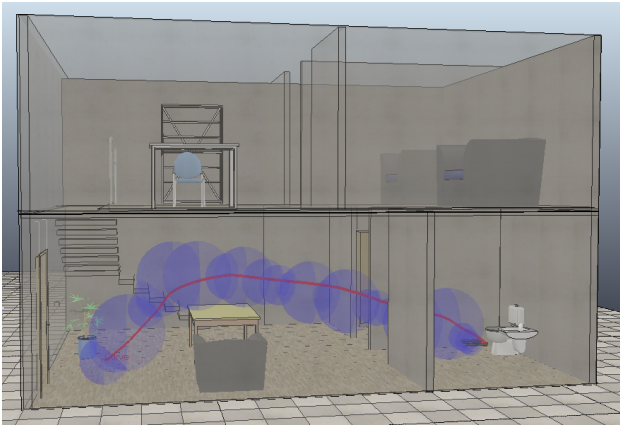


Figure 6. Simulation with the UAV for the path obtained by Experiment 1 considering one floor. The purple spheres represent the rosary and the red line is the trajectory performed by the UAV.

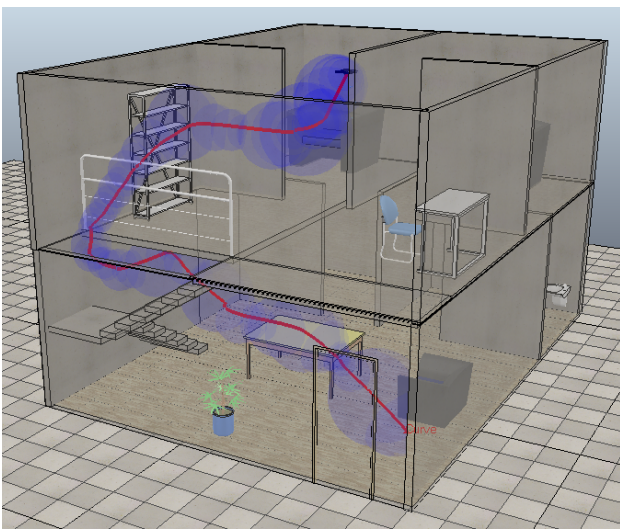


Figure 7. Simulation with the UAV for the path obtained by Experiment 2 considering two floors. The purple spheres represent the rosary and the red line is the trajectory performed by the UAV.

In these simulations, it was possible to observe the mentioned advantage of the rosary structure. During the entire UAV trajectory (red line), there was no part of the robot outside the bubbles, even when the UAV performs some maneuvers to follow the path. Thus, the UAV was capable of performing the entire indoor mission without colliding

with any obstacles. Besides, it also kept distance from the obstacles, proving the practicability of the method for this application.

Considering that GBPF is a stochastic algorithm, the method was performed 100 times (for both presented scenarios) in order to analyze the processing time (Time), the number of generated bubbles (Bubbles), and the length (Path) of the obtained path. Table 1 presents the average results for these simulations.

Table 1. Numerical results of processing time, number of bubbles, and path length for many simulations with the GBPF.

Apartment floors	Time (s)		Bubbles		Path (m)	
	avg	std	avg	std	avg	std
1st floor	0.554	0.544	252.280	149.998	11.136	1.276
1st and 2nd	2.091	0.786	923.600	183.110	21.898	2.024

The information shown in Table 1 is similar to the simulation results previously presented, which shows that the method is in accord with the simulations performed. Besides, it is possible to note that the method was capable of finding paths in a relatively short time and that no errors were found in any of the experiments.

## 5. CONCLUSION

This work presented an application of the Goal-biased Probabilistic Foam for generating paths for an Unmanned Aerial Vehicle to navigate in indoor missions. By using a structure called bubble, the method created a path considering only the free-space region, ensuring a safe motion for the UAV.

The approach used for computing the bubble made feasible paths, with high clearance from the obstacles. Besides, this bubble enabled GBPF to plan paths without the need for the obstacles explicit representation in the configuration space (C-obstacle), which would make this application computationally impracticable for complex scenarios.

Considering that the path planning strategy was executed in Matlab and the UAV motion simulation was performed in V-REP, it was necessary an approximated representation of the scene. In this sense, as future works, we suggest the implementation of a mapping system using consolidated techniques, which can expand the studies for local planning in real-time.

Finally, this work brought some early results for the application of Probabilistic foam-based path planning methods for UAV motion. For future research, we intend to compare these results with some state-of-the-art path planning algorithms for this application. Furthermore, we also seek to investigate strategies that allow safe navigation for autonomous multi-UAV systems.

## REFERENCES

- Aggarwal, S. and Kumar, N. (2020). Path planning techniques for unmanned aerial vehicles: A review, solutions, and challenges. *Computer Communications*, 149, 270–299.

- Berglund, T., Brodnik, A., Jonsson, H., Staffanson, M., and Soderkvist, I. (2009). Planning smooth and obstacle-avoiding b-spline paths for autonomous mining vehicles. *IEEE Transactions on Automation Science and Engineering*, 7(1), 167–172.
- Canny, J. (1988). *The complexity of robot motion planning*. MIT press.
- Chien, R.T., Zhang, L., and Zhang, B. (1984). Planning collision-free paths for robotic arm among obstacles. *IEEE Transactions on Pattern Analysis and Machine Intelligence*, PAMI-6(1), 91–96. doi:10.1109/TPAMI.1984.4767480.
- Grzonka, S., Grisetti, G., and Burgard, W. (2009). Towards a navigation system for autonomous indoor flying. In *2009 IEEE International Conference on Robotics and Automation*, 2878–2883. IEEE.
- Ju, C. and Son, H.I. (2018). Multiple uav systems for agricultural applications: control, implementation, and evaluation. *Electronics*, 7(9), 162.
- Jung, J., Yoo, S., La, W.G., Lee, D.R., Bae, M., and Kim, H. (2018). Avss: Airborne video surveillance system. *Sensors*, 18(6), 1939.
- La Scalea, R., Rodrigues, M., Osorio, D.P.M., Lima, C., Souza, R.D., Alves, H., and Branco, K.C. (2019). Opportunities for autonomous uav in harsh environments. In *2019 16th International Symposium on Wireless Communication Systems (ISWCS)*, 227–232. IEEE.
- LaValle, S.M. (1998). Rapidly-exploring random trees: A new tool for path planning.
- LaValle, S.M. (2006). *Planning Algorithms*. Cambridge University Press, New York, NY, USA.
- Lavalle, S.M., Kuffner, J.J., and Jr. (2000). Rapidly-Exploring Random Trees: Progress and Prospects. In *Algorithmic and Computational Robotics: New Directions*, 293–308.
- Ma, R., Wang, R., Liu, G., Chen, H.H., and Qin, Z. (2020). Uav-assisted data collection for ocean monitoring networks. *IEEE Network*, 34(6), 250–258.
- McCabe, B., Hamledari, H., Shahi, A., Zangeneh, P., and Azar, E.R. (2017). Roles, benefits, and challenges of using uavs for indoor smart construction applications. In *Computing in Civil Engineering 2017*, 349–357.
- Nascimento, L.B.P., Pereira, D.S., Sanca, A.S., Eugenio, K.J.S., Fernandes, D.H.S., Alsina, P.J., Araujo, M.V., and Silva, M.R. (2018a). Safe path planning based on probabilistic foam for a lower limb active orthosis to overcoming an obstacle. In *2018 Latin American Robotic Symposium, 2018 Brazilian Symposium on Robotics (SBR) and 2018 Workshop on Robotics in Education (WRE)*, 413–419. doi:10.1109/LARS/SBR/WRE.2018.00080.
- Nascimento, L.B.P., Barrios-Aranibar, D., Alsina, P.J., Santos, V.G., Fernandes, D.H.S., and Pereira, D.S. (2020). A smooth and safe path planning for an active lower limb exoskeleton. *Journal of Intelligent & Robotic Systems*, 99(3). doi:https://doi.org/10.1007/s10846-019-01134-7.
- Nascimento, L.B.P., Pereira, D.S., Alsina, P.J., Silva, M.R., Fernandes, D.H.S., Roza, V.C.C., and Sanca, A.S. (2018b). Goal-biased probabilistic foam method for robot path planning. In *Autonomous Robot Systems and Competitions (ICARSC), 2018 IEEE International Conference on*, 199–204. IEEE.
- Plaku, E., Plaku, E., and Simari, P. (2018). Clearance-driven motion planning for mobile robots with differential constraints. *Robotica*, 36(7), 971–993. doi:10.1017/S0263574718000164.
- Quinlan, S. (1995). *Real-Time Modification of Collision-Free Paths*. Doctoral dissertation, Stanford University Stanford, CA.
- Shakeri, R., Al-Garadi, M.A., Badawy, A., Mohamed, A., Khattab, T., Al-Ali, A.K., Harras, K.A., and Guizani, M. (2019). Design challenges of multi-uav systems in cyber-physical applications: A comprehensive survey and future directions. *IEEE Communications Surveys & Tutorials*, 21(4), 3340–3385.
- Takahashi, O. and Schilling, R.J. (1989). Motion planning in a plane using generalized voronoi diagrams. *IEEE Transactions on Robotics and Automation*, 5(2), 143–150. doi:10.1109/70.88035.
- Volna, E. and Kotyrba, M. (2018). Pathfinding in a dynamically changing environment. In N.T. Nguyen, D.H. Hoang, T.P. Hong, H. Pham, and B. Trawiński (eds.), *Intelligent Information and Database Systems*, 265–274. Springer International Publishing, Cham.
- Zhang, G., Shang, B., Chen, Y., and Moyes, H. (2017). Smartcavedrone: 3d cave mapping using uavs as robotic co-archaeologists. In *2017 International Conference on Unmanned Aircraft Systems (ICUAS)*, 1052–1057. IEEE.
- Zhao, Y., Zheng, Z., and Liu, Y. (2018). Survey on computational-intelligence-based uav path planning. *Knowledge-Based Systems*, 158, 54–64.